DR LINGLING ZHU (Orcid ID : 0000-0003-0489-0680)
DR SHINICHI ASAO (Orcid ID : 0000-0002-0334-5464)
PROF. MARK G TJOELKER (Orcid ID : 0000-0003-4607-5238)
PROF. PATRICK MEIR (Orcid ID : 0000-0002-2362-0398)
PROF. OWEN K ATKIN (Orcid ID : 0000-0003-1041-5202)

Article type : Regular Manuscript

Title: Acclimation of leaf respiration temperature responses across thermally contrasting biomes

AUTHORS: LINGLING ZHU[1, 2], KEITH J. BLOOMFIELD[1, 3], SHINICHI ASAO[1], MARK G. TJOELKER[4], JOHN J.G. EGERTON[5,6], LUCY HAYES[1], LASANTHA K. WEERASINGHE[5,7], DANIELLE CREEK[4, 5, 8], KEVIN L. GRIFFIN[9], VAUGHAN HURRY[10], MICHAEL LIDDELL[11], PATRICK MEIR[5], MATTHEW H. TURNBULL[12] AND OWEN K. ATKIN[1, 5*]

Affiliations:

[1]ARC Centre of Excellence in Plant Energy Biology, Research School of Biology, Building 134, The Australian National University, Canberra, ACT 2601, Australia

[2]College of Life Sciences and Oceanography, Shenzhen University, Shenzhen 518060, People's Republic of China

[3]Department of Life Sciences, Imperial College London, Silwood Park Campus, Buckhurst Road, Ascot SL5 7PY, UK

[4]Hawkesbury Institute for the Environment, Western Sydney University, Locked Bag 1797, Penrith, NSW 2751, Australia

This article has been accepted for publication and undergone full peer review but has not been through the copyediting, typesetting, pagination and proofreading process, which may lead to differences between this version and the Version of Record. Please cite this article as doi: 10.1111/NPH.16929

[5]Division of Plant Sciences, Research School of Biology, Building 46, The Australian National University, Canberra, ACT 2601, Australia

[6]Division of Ecology and Evolution, Research School of Biology, Building 116, The Australian National University, Canberra, ACT 2601, Australia

[7]Faculty of Agriculture, University of Peradeniya, Peradeniya, 20400 Sri Lanka

[8]INRAE Univ. Clermont-Auvergne, PIAF, 63000 Clermont-Ferrand, France

[9]Department of Earth and Environmental Sciences, Columbia University, Palisades NY, 10964, USA

[10]Umeå Plant Science Centre, Department of Forest Genetics and Plant Physiology,

Swedish University of Agricultural Sciences, Umeå SE-901 84, Sweden

[11]Centre for Tropical Environmental and Sustainability Science (TESS) and College of Science and Engineering, James Cook University, Cairns, QLD 4878, Australia

[12]Centre for Integrative Ecology, School of Biological Sciences, University of Canterbury, Private Bag 4800, Christchurch 8140, New Zealand

Correspondence: Owen Atkin; owen.atkin@anu.edu.au; Phone: +61 02 61255046

Received: *16 June 2020*

Accepted: *1 September 2020*

ORCID

LINGLING ZHU ORCID 0000-0003-0489-0680

SHINICHI ASAO ORCID 0000-0002-0334-5464

MARK G. TJOELKER ORCID 0000-0003-4607-5238

DANIELLE CREEK ORCID 0000-0002-8242-2359

KEVIN L. GRIFFIN ORCID 0000-0003-4124-3757

VAUGHAN HURRY ORCID 0000-0001-5151-5184

MICHAEL LIDDELL ORCID 0000-0001-9754-8184

PATRICK MEIR ORCID 0000-0002-2362-0398

MATTHEW H. TURNBULL ORCID 0000-0002-3433-5859

OWEN K. ATKIN ORCID 0000-0003-1041-5202

Summary

- Short-term temperature response curves of leaf dark respiration (*R*-*T*) provide insights into a critical process that influences plant net carbon exchange. This includes how respiratory traits acclimate to sustained changes in the environment.
- Our study analyses 860 high-resolution *R*-*T* (10–70°C range) curves for: (a) 62 evergreen species measured in two contrasting seasons across several field sites/biomes; and (b) 21 species (sub-set of those sampled in the field) grown in glasshouses at 20/15, 25/20 and 30/25 °C (day/night).
- In the field, across all sites/seasons, variations in R_{25} (measured at 25 °C) and the leaf-*T* where *R* reached its maximum (T_{max}) were explained by growth-*T* (mean air-*T* of 30-days prior to measurement), solar irradiance and vapor pressure deficit, with growth-*T* having the strongest influence. R_{25} decreased and T_{max} increased with rising growth-*T* across all sites and seasons with the single exception of winter at the cool-temperate rainforest site where irradiance was low. The glasshouse study confirmed that R_{25} and T_{max} thermally acclimated.
- Collectively, the results suggest: (1) thermal acclimation of leaf *R* is common in most biomes; and, (2) the high-*T* threshold of respiration dynamically adjusts upward when plants are challenged with warmer and hotter climates.

Key words: climate change; metabolism; phenotypic plasticity; respiration modelling; thermal acclimation; thermal tolerance.

Introduction

In recent decades, increasing efforts have been made to describe respiratory responses to temperature (*T*) in a wide range of organisms (Dahlhoff *et al.*, 1991; Dahlhoff & Somero, 1993; O'Sullivan *et al.*, 2013; Padfield *et al.*, 2016; O'Sullivan *et al.*, 2017). A key method used in studying plants has been the use of high resolution short-term *T*-response curves to characterise the impact of changes in the thermal environment on rates of respiratory CO_2 release in darkness (*R*-*T* curves) (O'Sullivan *et al.*, 2013; Heskel *et al.*, 2016; Padfield *et al.*, 2016; O'Sullivan *et al.*, 2017). Such curves provide evidence that leaf *R* (leaf respiration) adjusts to sustained changes in growth *T,* with the trans-continental coverage of *R*-*T* curves increasing our understanding of global patterns of leaf *R*. They have also enabled better design of ecosystem and land surface models that predict the impacts of possible future thermal regimes on plant communities (Arora *et al.*, 2013; Dufresne *et al.*, 2013; Huntingford *et al.*, 2017). Leaf *R*-*T* curves also provide insights into the thermal limits of leaf energy metabolism by measuring respiratory responses to very high and potentially lethal temperatures (Hüve *et al.*, 2012; O'Sullivan *et al.*, 2013; O'Sullivan *et al.*, 2017).

When assessing how seasonal variations in climate might affect leaf *R*, we need to consider how respiratory metabolism acclimates to sustained changes in growth *T*. Thermal acclimation can result in warm-grown plants exhibiting lower rates of leaf *R,* at a given measuring *T*, compared to their cold-grown counterparts (Atkin & Tjoelker, 2003; Slot & Kitajima, 2015). By reducing the rates of leaf *R* in warm-grown plants, acclimation could dampen the effects of sustained warmer *T* on respiratory CO_2 release, moderating an anticipated positive feedback loop between climate warming and CO_2 efflux from terrestrial plants (Smith & Dukes, 2013; Smith *et al.*, 2015; Huntingford *et al.*, 2017).

If thermal acclimation of *R* is widespread in the plant kingdom, it should be accounted for when predicting the effects of temporal variations in climate on terrestrial ecosystem net carbon exchange. In a review of 43 studies of mostly controlled-environment studies of warm- and cool-grown plants (103 species), Slot and Kitajima (2015) found that leaf *R* at a given *T* is often downregulated in warm-grown plants relative to those grown at lower *T*. Subsequent studies have reported similar patterns (Aspinwall *et al.*, 2016; Drake *et al.*, 2016; Reich *et al.*, 2016; Benomar *et al.*, 2017; Drake *et al.*, 2019). One way of doing this is to assume that comparisons of cool- *vs* warm-grown plants (e.g. comparing plants in controlled environments or field-grown plants from thermally-contrasting biomes) can be used to model

the response of leaf *R* to seasonal changes in growth *T* and/or future global warming (Smith *et al.*, 2015; Vanderwel *et al.*, 2015).

A five-year study by Reich *et al.* (2016) reported consistent thermal acclimation of 10 boreal and temperate tree species saplings to both *in situ* warming and seasonal changes in growth *T* over the spring to late summer. Likewise, leaf *R* acclimates to both *in situ* experimental warming and seasonal *T* changes of similar magnitude in *Eucalyptus tereticornis* trees grown under temperate field conditions (Aspinwall *et al.*, 2016). However, seasonal field measurements of leaf *R* across contrasting biomes are rare. Most studies quantifying thermal acclimation have compared cool- and warm-developed plants that were either grown under controlled environment conditions, or field conditions that included manipulation of growth *T* via *in situ* warming. Moreover, most field-based studies have been limited to a single site or single species (Atkin *et al.*, 2000; Bruhn *et al.*, 2007; Tjoelker *et al.*, 2009; Dillaway & Kruger, 2011; Way *et al.*, 2015; Araki *et al.*, 2017; Asao *et al.*, 2020), limiting our ability to directly compare thermal acclimation of *R* in contrasting biomes. This is particularly the case for evergreen ecosystems, where seasonal data on mature trees are scarce. In such ecosystems, leaves not only experience seasons marked by changes in growth *T*, but also water availability and daily irradiance that could influence *R* (Atkin *et al.*, 1998; Gauthier *et al.*, 2014).

Conducted over a wide range of measuring *T* (e.g. usually between 5 to 45 °C), high resolution leaf *R*-*T* curves can be used to derive *T*-response parameters such as the proportional change per 10 °C rise in *T* (Q_{10}), activation energy (E_a) (Kruse *et al.*, 2011) or 2nd order polynomial model coefficients (Heskel *et al.*, 2016; Liang *et al.*, 2018). Heskel *et al.* (2016) reported on high-resolution *R*-*T* curves made at 18 sites across the globe (single season only) and found that the temperature response of leaf *R* is generalizable across biomes and plant functional types using fixed values of parameters in 2nd order polynomial models. Using this approach, natural log transformed (*ln*) rates of *R* are related to *T* according to:

$$ln\ R = a + b\mathrm{T} + c\mathrm{T}^2 \qquad \text{(Eqn 1)}$$

where *a, b* and *c* are coefficients that minimize residuals in the polynomial model. What remains unclear, however, was whether the shape of *R*-*T* curves (as indicated by the *b* and *c* terms) remains constant across seasons within sites (and, therefore, is constant through time).

When leaves are heated beyond 45 °C, leaf *R* sometimes shows a spike until rates peak at a maximal value, followed by a rapid irreversible decline as cell membranes lose integrity and proteins begin to denature (O'Sullivan *et al.*, 2013; O'Sullivan *et al.*, 2017); this high-temperature threshold of leaf *R* is here termed 'T_{max}'. In plants, T_{max} values of leaf *R* are

typically in the 50-60 °C range, being highest in hot biomes (O'Sullivan *et al.*, 2017). The T_{max} of leaf *R* increases linearly with decreasing latitude, being *ca.* 8 °C higher in equatorial tropical forests than in the high latitude, arctic tundra (O'Sullivan *et al.*, 2017). There is also some evidence that T_{max} acclimates to sustained increases in seasonal *T* (O'Sullivan *et al.*, 2017) or heatwaves (Aspinwall *et al.*, 2019), and that factors such as drought can influence T_{max} (Gauthier *et al.*, 2014). Whether the reported seasonal patterns are maintained across a wider range of biomes is not known. Furthermore, the extent to which T_{max} acclimates to changes in growth *T* has not yet been tested in a wide range of species under controlled-environment conditions where the effects of air temperature can be isolated from potential confounding factors observed in the field.

In this study, we measured 860 high-resolution leaf *R*-*T* curves (typically with *T* ramped from 10 – 70 °C at 1 °C min^{-1}, Fig. S1) in a wide range of evergreen plant species adapted to thermally contrasting biomes across Australia; biomes included arid woodlands, temperate woodlands, temperate wet forests, and tropical rainforests. Our study evaluated the impact of the thermal environment on the leaf trait characteristics (e.g. *R* at a given measuring *T* and T_{max}) of leaf *R*-*T* curves by making measurements in two climatically-distinct seasons at six field sites, and by growing a subset of these same species under temperature-controlled glasshouse conditions. We tested the generality of glasshouse responses by comparing them to the responses in the field. Our study tested the hypothesis (as described in Figure 1) that - regardless of whether comparing field grown plants from multiple sites/seasons or glasshouse grown plants developed under contrasting temperatures - warm-grown plants, compared to their cooler-grown counterparts, would exhibit: (i) lower rates of leaf R_{25} (*R* measured at 25°C), with R_{25} scaling negatively with increasing growth *T*; (ii) higher T_{max} values, with T_{max} scaling positively with increasing growth *T*; and, (iii) no change in the shape of the *R*-*T* curves - i.e., no change in the value of the temperature coefficients *b* and *c* in the 2nd order polynomial model fitted to log *R*-*T* curves (Heskel *et al.*, 2016).

Materials and methods

Field site description and species sampling

We chose six sites from thermally contrasting biomes across Australia (Tables 1 and S1): two tropical rainforest sites, Cape Tribulation and Robson Creek, are located in Far North Queensland (FNQ_CT and FNQ_RC); arid woodland, Alice Mulga, in the Northern Territory (NT_AM); Mediterranean woodland, Great Western Woodland, in Western Australia

(WA_GWW); temperate forest, Cumberland Plain in New South Wales (NSW_CP); and, temperate rainforest, Warra, in Tasmania (TAS_WAR). All sites belong to the Terrestrial Ecosystem Research Network [for more information on the sites refer to Karan *et al.* (2016), Bloomfield *et al.* (2018) and Zhu *et al.* (2018)]. Mean annual temperatures (MAT) range from 9.8 to 24.3 °C; mean annual precipitation ranges from 291 mm to 3671 mm (Table S1).

At each site, 1-2 week campaigns were conducted in two separate seasons (refer to Table 1 for climate data in the 30-day period leading up to each campaign). The timing of campaigns was designed to maximise seasonal environmental differences at each site. We chose ~10 of the most abundant evergreen species at each site, with four or five replicate individuals, one leaf per individual; in total, 62 species were sampled. Repeat sampling was made on the same individual for more than 80% of individuals in WA_GWW and NSW_CP. At other sites, the original plant could not be identified with certainty on the repeat visit; nevertheless, trees sampled in the two seasons were in close proximity to each other, sharing similar microclimates and soil. Upper canopy, sun-lit branches were excised from mature plants in the morning or early afternoon and the stems immediately re-cut under water and stored in cool, moist dark conditions until measurements, which occurred within six hours of sampling.

Controlled environment study

The controlled environment study followed the experimental set up of a companion study described in Zhu *et al.* (2018); seedlings of 26 species (Table S2) were grown in a glasshouse at the Research School of Biology, Australian National University, Canberra, Australia. All species had been included in the earlier field sampling. Nineteen species were obtained as seedlings from local nurseries near each field site (refer to Table S2 for provenances and climate details). The remaining seven species were unavailable from local nurseries and were purchased as seeds from a commercial supplier and planted in a glasshouse four months prior to obtaining seedlings for the rest of study species. The selected species represent four general provenances or origins close to the field sites: FNQ - Tropical rainforests; NSW - Temperate forest; TAS - Temperate rainforest; WA - Mediterranean woodland. Provenance details are shown in Table S2. When first purchased, seedlings were 30–50 cm in height similar to the seedlings cultivated from seeds. They were then re-potted into 18 x 18 x 25 cm free-draining pots containing organic potting mix, enriched with Osmocote® OSEX34 EXACT standard slow-release fertiliser (Scotts Australia, Bella Vista, NSW) and 30% river sand. Plants were well-watered daily.

The glasshouse study consisted of two stages. In Stage 1, all plants were grown for two months under a single temperature treatment (25/20 °C day/night) under natural photoperiod conditions to assess whether there were inherent differences in the shape of *R*-*T* curves of the 26 selected species. In Stage 2, plants initially grown in Stage 1 were separated into two groups to assess the capacity of individual species to acclimate to lower and higher growth temperatures by exposing plants to two growth temperature treatments (20/15 °C and 30/25 °C day/night). Statistical analyses were conducted separately for the two experimental stages.

In Stage 1, seedlings were arranged using a split-block design in three adjacent glasshouses. A total of 260 plants (26 species × 5 replicates × 2 adjacent individual plants) were located in five replicate blocks. Species were randomly placed within sub-blocks, and sub-blocks were positioned randomly within each block. For each species, two individuals were placed adjacent to each other side-by-side to facilitate subsequent separation of plants into cooler and warmer growth temperatures (i.e. Stage 2). Sampling for Stage 1 measurements started after two months of growth in the 25/20 °C treatment and using newly developed foliage. One of the two adjacent individuals from each block was measured; thus, a total of 130 measurements (i.e. 26 species x 5 blocks) were made for Stage 1. The timing of sampling of each species/replicate combination was randomized (both within and between days). Measurements of *R*-*T* curves and associated traits were made over a 20-day period in winter (June) 2015 when day-length was *ca.* 10 hours (14 h night), at least two hours after sunrise and one hour before sunset. No significant differences for any *R*-*T* parameters were found among the five replicate blocks distributed across the three glasshouses ($P > 0.6$ for all parameters), indicating a lack of block effect on *R*-*T* responses.

In Stage 2, we assessed whether the shape of *R*-*T* curves differed between leaves developed under warmer (30/25 °C) and colder (20/15 °C) temperatures. Using plants sourced from Stage 1, 168 plants (i.e. 21 species x two treatments x four replicates) were measured; a smaller number replicates were sampled in Stage 2 because of the low variability in *R*-*T* curve derived parameters among replicate blocks observed in Stage 1 and the requirement for increased sampling constraints (two treatments instead of one). Two of the original three glasshouses were used for Stage 2, and temperatures were adjusted to 30/25 °C and 20/15 °C. The two adjacent individuals of the same species in each block in Stage 1 were moved to the two glasshouses, with individuals randomly arranged within four blocks. Measurements of *R*-*T* curves commenced 20 days after adoption of the new temperature regimes. In most cases, fully expanded, newly-matured leaves that formed under the new

growth conditions were used for *R-T* measurements except for three acacia species (*A. anuera*, *A. burkitti* and *A. hemetelis*), where pre-existing mature foliage was used. As with Stage 1, the sampling sequence of each treatment/genotype/block was randomized. Measurements took place in spring (October) 2015 over a 15-day period when average day-length was *ca*.13 hours.

Temperature responses of leaf dark respiration

Detached, whole leaves from sun-exposed, new, fully-expanded foliage were used for measurements, sampled either from cut branches (in the field) or directly from plants (controlled environments). Note: for a few species such as *Hakea* and *Melaleuca*, individual leaves were too small for measurements. In those cases, the most recently mature, fully expanded parts of whole shoots were used. In all cases, leaves were placed in a Peltier system chamber (20 cm length x 8 cm width x 5 cm height, 3010-GWK1 Gas-Exchange Chamber, Walz, Heinz Walz GmbH, Effeltrich, Germany) and kept in dark for about 30 min before data recording. The chamber was as an open system connected to a LiCor unit (LI-6400XT; Li-Cor Inc., Nebraska, USA) with controlled CO_2 supply (set to the prevailing ambient concentration) and a flow rate of 500 μmol s^{-1}. During the 30 min dark-adaptation period in each chamber, air temperature was cooled (to 10°C in most cases, except for measurements in hot conditions where the lowest temperature was in the range of 15-20 °C). Once cooled, leaves were heated continuously at a rate of 1 °C min^{-1} up to 60-70 °C. Because these measurements took place in dark, vapour pressure deficit (VPD) effects on stomatal conductance were not considered relevant. Leaf temperature was recorded every second using a small-gauge wire copper constantan thermocouple pressed against the underside of the leaf. Respiratory CO_2 efflux rates were recorded every 30 s, with lags from respiration in the mitochondria to measurement site assumed to be minimal. After each run, the measured leaf was removed from the cuvette, placed in a drying oven at 65 °C for a minimum of three days and weighed.

No leaf desiccation was observed when leaves were heated up to 45 °C. However, as leaves heated to 60-70 °C in the 3010-GWK1 chamber became desiccated and shrunk, an adjacent leaf to that used for the *R-T* curves was sampled for measurement of fresh mass, after which leaves were photo-scanned. The scanned images were used to calculate leaf area using *Image J* (www://imagej.nih.gov/ij/). As was the case with *R-T* leaves, adjacent leaves were oven dried (65 °C for 3 days). The ratio of leaf dry mass to leaf area (LMA) was calculated for the adjacent leaves and were then used to inter-convert area-based values of the

T leaves. These same dried, adjacent leaves were subsequently used for nitrogen analyses. For species whose whole shoots were used for *R*-*T* curves, separated leaves and stems were scanned and only the area of leaves was used in the calculation of LMA and nitrogen analysis.

Nitrogen analyses

Total nitrogen concentration in the adjacent leaves was measured using the Kjeldahl method (Novozamsky *et al.*, 1974). Oven dried leaf tissues were ground then digested using 98% sulfuric acid at 350 °C. The concentration was determined using a LaChat Quikchem 8500 Series 2 flow injection system (Lachat Instruments, Milwaukee, WI, USA).

Climate data

For climate variables specific to each site when the plants were measured, climate data (30 min resolution) were obtained from the eddy covariance flux tower at each site (Beringer *et al.*, 2016). This was not possible for the two earliest campaigns, which preceded tower construction (dry season at FNQ_RC, and summer at TAS_WAR) where climate data (temperature and precipitation) were estimated using the ANUClimate model (Hutchinson *et al.*, 2009). For the controlled environment study, long-term climate data were obtained from the Atlas of Living Australia (ALA) (www.ala.org.au, sourced March, 2016) based on the provenances of each species provided by the nurseries or seed supplier. Climate data from ALA records were extracted using ANUCLIM V6 (Xu & Hutchinson, 2011).

Data analysis

Each leaf *R*-*T* curve was used to calculate R_{25} (i.e. *R* at 25 °C), rate-temperature coefficients and T_{max} (Fig. 1, Fig. S1). R_{25} was expressed on leaf area, dry mass and leaf N bases (R_{25a}, R_{25m} and R_{25n}, respectively). For *T* response models, a 2nd order polynomial curve (see Eqn 1 in the Introduction) was fitted to a plot of log *R* vs *T*, using data up to 45 °C (O'Sullivan *et al.*, 2013; Heskel *et al.*, 2016). Data beyond 45 °C were excluded for model fits as there is often a 'burst' in respiration at *T*s > 45 °C (O'Sullivan *et al.*, 2013). Here, the *a* parameter indicates extrapolated values of ln *R* at 0 °C, *b* is the slope of ln *R* vs. *T* plot at 0 °C, and *c* represents quadratic nonlinearity in the ln *R* vs *T* slope. *b* and *c* are the rate-temperature coefficients. T_{max} was calculated as the temperature where respiration reaches the maximum rate before irreversibly declining; in most experiments, this was at leaf *T*s > 55 °C.

For field data, linear mixed-effects models and analysis of variances (ANOVA) models were used to compare differences in LMA, N_m (mass-based concentrations of leaf nitrogen),

R_{25a}, R_{25m}, R_{25n}, b, c and T_{max}, with site and season and their interaction as fixed effects, and species and plant replicates (individuals) as random effects. Field data were separated into individual sites and analysed using linear mixed-effects models with season as fixed effects and species, replicates as random effects and ANOVA was also performed. Mean T, mean VPD, mean net radiation (F_n) and total precipitation (PPT) of the 30 days period prior to the date of measurements (PDM) were calculated. Variance inflation factors for the above four parameters were below 5.0, suggesting collinearity between them were not an issue. Backwards-stepwise regressions were performed between selected R-T parameters and mean T, PPT, VPD and F_n of the 30 days PDM. We chose 30 days, as this period is likely to be sufficient for full acclimation for leaf metabolic processes (Atkin *et al.*, 2000; Cunningham & Read, 2003; Zaragoza-Castells *et al.*, 2007; Reich *et al.*, 2016).

For the glasshouse Stage 1 experiment, a split-block design ANOVA was used to assess differences among biome origins for LMA, N_m, R_{25a}, R_{25m}, R_{25n}, b, c and T_{max}. For the glasshouse Stage 2 experiment, a linear mixed-effects model and ANOVA were used to compare differences in LMA, N_m, R_{25a}, R_{25m}, R_{25n}, b, c and T_{max} among origins and growth temperature, with biome origin and temperature treatment as fixed effects and species and plant replicates (individuals) as random effects. In addition, for each biome origin, a linear mixed-effects model and ANOVA were used to compare differences between the two temperature treatments, with temperature treatment and species as fixed effects and replicates as random effects.

For both field and glasshouse Stage 2 experiments, linear mixed-effects models were used to partition trait variation by assigning all categorical factors (biome origin, site, species, treatment) as random terms. Linear mixed-effects models were also performed to predict values of R_{25a} and T_{max} at a species level, with growth T (for field, growth T was the mean T of 30 days PDM; for the glasshouses, growth T was the daily mean T value) as a fixed effect, and species and experimental setting (field / glasshouse) as random effects. Both random intercepts and random slopes were included for random effects in the mixed-effects models. Non-normal distributed data (LMA, N_m, R_{25a}, R_{25m}, R_{25n}, and climate variables) were log-transformed and statistics were performed in R, the "lmer" function in the "lme4" package was used for the linear mixed-effects model (Bates *et al.*, 2014; R Development Core Team, 2020).

Results

Leaf structure and chemical composition

In the field, LMA and N_m did not show any particular patterns. LMA and N_m exhibited significant site-by-season interactions (Table 2). LMA was significantly higher in winter than summer at site NSW_CP but lower in winter than summer at TAS_WAR (Fig. 2A). N_m was significantly higher in the cool or dry season at FNQ_CT and FNQ_RC but significantly lower in winter than summer at WA_GWW (Fig. 2B).

In the glasshouse study, LMA was significantly higher in plants grown in 20/15 °C than 30/25 °C for all four biome origins, while N_m did not respond to the two *T* treatments (Fig. 2C & 2D; Table 3). Both LMA and N_m differed significantly among the four biome origins in both Stage 1 (Table S3) and Stage 2 (Table 3) experiments, with LMA and N_m being highest in species whose origin was WA (Fig. 2C & 2D).

Acclimation of *R-T* parameters in the field

In the field, season affected leaf respiration rates expressed on a per unit leaf area (R_{25a}), dry mass (R_{25m}) and nitrogen (R_{25n}) basis, as well as the *T* at which maximal rates of leaf *R* occurred (T_{max}) (all $P < 0.01$); by contrast, season did not affect *b* and *c* ($P > 0.5$). All *R-T* parameters (R_{25a}, R_{25m}, R_{25n}, *b*, *c* and T_{max}) exhibited significant site-by-season interactions (Table 2). Given this, the effect of season was assessed at each site separately. Consistent with the pattern predicted in Figure 1, R_{25a} was significantly higher in the cool (i.e. winter) than warm (summer) season at four of the six sites (FNQ_CT, FNQ_RC, WA_GWW and NSW_CP; Fig. 3A). Unexpectedly, R_{25a}, R_{25m} and R_{25n} were significantly lower in winter than summer at TAS_WAR (Figs 3A, B & C).

To assess relationships between climate and parameters derived from *R-T* curves, we plotted species mean values of R_{25a} against a range of abiotic factors recorded over the 30 days period prior to the date of measurements (PDM) in winter and summer (Fig. 4). The climate variables assessed were: (a) mean daily *T*; (b) mean daily net radiation (F_n); (c) mean daily atmospheric vapour pressure deficit (VPD); and, (d) total precipitation (PPT) of the 30 day PDM. To further assess whether variations in R_{25a} are linked to variations in these climate factors, we firstly performed linear regressions to assess relationships between R_{25a} and each climate variables individually (Fig. 4). R_{25a} increased with F_n ($r^2 = 0.139$, $P < 0.001$), and VPD ($r^2 = 0.192$, $P < 0.001$), with winter and summer sharing common slopes

but differing in intercepts (Fig. 4, Table S4). R_{25a} declined with PPT similarly in both seasons ($r^2 = 0.204$, $P < 0.001$). To further explore the linkages between R_{25a} and climate, we used stepwise multiple regressions (Table 4) to assess three scenarios: (1) all site and season data; (2) all data but excluding summer and winter TAS_WAR data because this site showed an pattern different from the main body of data; and, (3) all data but excluding winter only TAS_WAR data. When all sites and seasons (scenario a) were included, 31% of the variation of R_{25a} was explained by variations in mean daily T, F_n and VPD (Fig. 3A, Table 4, $r^2 = 0.305$, $P < 0.001$). When excluding TAS_WAR summer and winter (scenario b) and winter alone (scenario c) data, only mean daily T and VPD were retained in the model (Table 4, excluding both summer and winter data, $r^2 = 0.298$, $P < 0.001$; excluding winter alone data, $r^2 = 0.288$, $P < 0.001$). Thus, so long as the low-light conditions of TAS_WAR in winter were excluded, *ca.* 30% of the variation in R_{25a} across all sites could be explained by variations in mean T and VPD alone, with variations in mean T being the dominant factor (as indicated by the *t*-value and *p*-value for each coefficient; Table 4). These results also point to the low winter values of F_n at TAS_WAR contributing to the low rates of R_{25} observed at that site.

T_{max} was significantly higher in the warm compared to cool season at four of the six sites (FNQ_RC, NT_AM, WA_GWW and NSW_CP; Fig. 3D). While T_{max} was significantly lower in the warm/wet season than the cool/dry season at the lowland tropical rainforest site (FNQ_CT), there was relatively little seasonal difference (0.6 °C) in mean T (Table 1) but a large difference between the wet season and dry season precipitation (1288mm, 210mm, respectively) over the 30 day PDM at this site. As was the case with R_{25a}, we plotted T_{max} against a range of abiotic factors recorded over the 30 days PDM in winter and summer (Fig. 4). In contrast to R_{25a}, T_{max} exhibited similar response patterns to seasonal changes in mean T and VPD across all sites, including TAS_WAR (Fig. 4E & 4G). Linear regression analyses revealed significant positive relationships between T_{max} and both mean T and F_n, with winter and summer sharing the same intercepts and slopes (Fig. 4E, F, Table S4). Significant linear regressions were also found between T_{max} and VPD, with summer and winter sharing the same slope but differing in intercepts (Fig. 4G, Table S4). Further, stepwise regressions – using data from all sites and seasons - showed that variations of T_{max} could be explained by variations in mean T, F_n and VPD (Table 4, $r^2 = 0.298$, $P < 0.001$). As was the case for R_{25a}, variations in mean daily T were the dominant factor contributing to variation in T_{max} (see *t*-value and *p*-value for each coefficient in Table 4).

At three of the six sites (FNQ_RC, WA_GWW and TAS_WAR), parameter *b* changed between the cool and warm seasons, but the direction of change differed among the sites (Fig. 3E). At two sites (WA_GWW and TAS_WAR), season also had a significant effect on *c* values (Fig. 3F), but with the direction of that effect differing between the two sites.

Acclimation of *R-T* parameters in the glasshouses

Similar to the results of the field study - when excluding winter at TAS_WAR - R_{25a} decreased with increasing growth *T* in the greenhouse as hypothesized in Figure 1. In the glasshouse, R_{25a}, R_{25m} and R_{25n} were higher in plants grown under cooler (20/15 °C) than warmer growth conditions (30/25 °C), with no interaction between origin and growth *T* treatment (Figs 5A, B & C; Table 3), pointing to an origin-wide response that was consistent with the pattern predicted in Figure 1. In both Stages 1 and 2 of the glasshouse experiment, R_{25a}, R_{25m} and R_{25n} differed significantly among biome origins (Table 3, Table S3). R_{25n} decreased with mean annual *T* of origin, and R_{25a}, R_{25m} with decreased with mean annual precipitation of biome origin (Fig. S3E, F, Table S5).

T_{max} increased with growth temperature (Fig. 5D, Table 3) but did not differ among origins (Table 3 & S3). To assess the extent of acclimation of T_{max} in the field and glasshouse studies, we calculated the degree to which T_{max} increased per °C rise in growth *T*. In general, the dependence of T_{max} on growth *T* was similar in the field and glasshouse studies, as predicted from linear mixed-effects models (Fig. 6B).

Variance partitioning (Fig. S2) revealed that in the field, season alone contributed very little to variation (< 1 % of total trait variation) in LMA, N_m, R_{25a}, R_{25m}, R_{25n}, *b* and *c*; season alone accounted for 8 % variation in T_{max}. For all traits other than the temperature-rate coefficients, species (i.e. an indication of the role of genotype) contributed substantially to trait variation in the field. In the glasshouse Stage 2 study, growth *T* treatment alone explained the following variation in: LMA (16 %), R_{25a} (20 %), R_{25m} (11 %), R_{25n} (16 %) and T_{max} (30 %). Growth temperature did not contribute to variation in N_m, *b* or *c* (< 1 %). Variance in all traits could be explained by biome origin to some degree (9 – 30 %), with the exception of T_{max} (< 1 %).

Discussion

Thermal acclimation of R_{25} – implications for ecosystem modelling

Our study found that in the field acclimation of R_{25a} generally occurs as hypothesized in Figure 1; a notable exception was the cool rainforest site TAS_WAR that showed significantly lower R_{25} in winter than summer, with extremely low solar irradiance likely accounting for the low rates of R_{25a} in winter at that site (Fig. 3A, 3B & 3C). In the glasshouse study, acclimation of R_{25} occurred as hypothesized in Figure 1 across species (Figs 5A-C & 6A). Interestingly, despite the evidence that respiration acclimated to seasonal changes in the environment at most sites (Figs 3 & 6), season as a factor contributed relatively little to overall variance of respiratory traits in the field (Fig. S2) – a finding that highlights the contribution of other factors, particularly differences in respiration rates among species. Importantly, R_{25a} scaled negatively with increasing growth T in both the field (when excluding winter data from TAS_WAR) and glasshouse surveys, pointing to a broadly consistent acclimation response to growth T of plants in the field via seasonal changes in growth T with similar results observed in glasshouse experiments where growth T was manipulated alone (Fig. 6A). Averaged across species, the degree of thermal acclimation of R_{25a} was -0.035 μmol CO_2 m^{-2} s^{-1} per °C increase in growth T in the field when excluding the winter TAS_WAR data, and -0.017 μmol CO_2 m^{-2} s^{-1} per °C for the glasshouse study. These values are close to the values reported in Reich *et al.* (2016), where the degree of acclimation varied between -0.017 to -0.030 μmol CO_2 m^{-2} s^{-1} per °C increase in the growing season T at cold-temperate boreal forest site. Taken together, these results point to thermal acclimation of leaf R being a consistent phenomenon that is manifested seasonally in the field and when individual plants experience contrasting growth T under controlled environment conditions. We also found the same relationship when comparing species growing in thermally contrasting field sites. The consistent nature of thermal acclimation suggests that it can be incorporated into ecosystem modelling frameworks for most biomes.

While many studies have reported seasonal variations in leaf R in the field that are consistent with the thermal acclimation hypothesis (Strain, 1969; Atkin *et al.*, 2000; Bruhn *et al.*, 2007; Tjoelker *et al.*, 2009; Ow *et al.*, 2010; Dillaway & Kruger, 2011; Searle *et al.*, 2011; Searle & Turnbull, 2011; Way *et al.*, 2015; Aspinwall *et al.*, 2016; Drake *et al.*, 2016; Reich *et al.*, 2016; Araki *et al.*, 2017; Benomar *et al.*, 2017; Turnbull *et al.*, 2017; Quan & Wang, 2018; Drake *et al.*, 2019; Li *et al.*, 2019), most were conducted using deciduous trees or

short-lived herbaceous plants. Moreover, such studies have been conducted over only a part of the year (e.g. from spring to late summer) where *T* is likely to be the primary factor limiting growth and metabolism. This left open the question of whether evergreen, long-lived leaves of angiosperms that experience marked shifts in the seasonal environment (where large changes in precipitation, VPD, light and temperature all occur) also exhibit changes in leaf *R* consistent with that shown in Figure 1. Our study showed acclimation patterns in Australian long-lived evergreen trees and shrubs that were generally consistent with that reported for deciduous trees or short-lived herbaceous plants, suggesting that seasonal thermal acclimation occurs in wide range of biomes and forest types.

When excluding winter observations at the cool temperate wet forest site in Tasmania (TAS_WAR), the overall pattern showed R_{25a} decreasing with increasing growth *T* in the field and glasshouse studies (Fig. 6A), as hypothesized in Figure 1. However, variations in R_{25a}, were also explained by the changes in net radiation (F_n) and vapour pressure deficit (VPD) of air across all sites and seasons (Table 4). When we excluded TAS_WAR, F_n was not retained in the model. This suggests that the extremely low R_{25a} in winter TAS was related, at least in part, to the extremely low light that occurs at this high latitude site (Fig. 4B). A temperate wet forest site in New Zealand also exhibited rates of leaf *R* that do not follow general patterns across a global scale (Atkin *et al.*, 2015). Shorter days and persistent low light in winter reduces the availability of light to drive photosynthesis; lower photosynthesis would in turn reduce the demand for respiratory products. Seasonal variation in carbon demand by developing tissues (i.e. carbon 'sinks') may also contribute to variations in leaf *R* of source leaves (Wright *et al.*, 2006), with low sink demand (e.g. reduced growth during the cold, low light period of winter) decreasing the demand for respiratory products in winter of TAS_WAR. Thus, while thermal acclimation is generally wide spread, modelling of seasonal changes in low light, high latitude wet temperate forests will require further work to understand how variations in photosynthesis and sink demand, influence seasonal variations in leaf *R*.

Our study also points to water availability and/or loss potentially playing a role in regulating rates of leaf *R*. We found that total precipitation (PPT) of 30 days prior to the date of measurement (PDM) in the field was negatively related to R_{25a} (Fig. 4D). Global surveys also reported that higher leaf R_{25} is associated with lower PPT (Wright *et al.*, 2004; Wright *et al.*, 2006; Atkin *et al.*, 2015). Further, R_{25a} exhibited a positive relationship with VPD (Fig. 4C), suggesting that leaf *R* increases under conditions of high potential water loss from leaves to the atmosphere. While these observations might simply be a result of leaves adjusting

rates of leaf R to deal with water availability/loss, our finding that rates of R_{25a} and R_{25m} were inherently higher in plants sourced from drier origins (Fig. S3E, F, Table S5) suggests that the field observations may have reflected a combination of inherent differences in rates of leaf R among species adapted to mesic vs arid conditions plus phenotypic adjustments that occur in response to low rainfall and/or high VPD. Interestingly, PPT was not retained in the stepwise regression analyses, with VPD (along with mean T and F_n) being retained in models (Table 4). Importantly, this presumed role of VPD is relatively minor compared to that of growth T, with mean T of the 30 days PDM being the major factor explaining variations in leaf R_{25a} in the field (Table 4).

Thermal acclimation of T_{max} - implications of respiratory heat tolerance

The current study found that in the field, acclimation of T_{max} occurred as hypothesized but with an exception of the tropical rainforest site FNQ_CT that showed significantly higher T_{max} in the dry/slightly cooler season (Fig. 3D). Acclimation of T_{max} was as hypothesized across species in the glasshouses (Fig. 5D) and across biomes including rainforest species from FNQ area. with field and glasshouse grown plants exhibiting similar acclimation patterns of T_{max} in response to growth T (Fig. 6B). These results strongly suggest T_{max} is highly plastic and is strongly regulated by a leaf's thermal history; further, our results revealed no evidence of inherent differences among species adapted to thermally contrasting conditions (Fig. S3D, Table S5).

The importance of growth T in driving shifts in T_{max} supports recent reports of thermal acclimation of respiratory heat tolerance (i.e. T_{max}) (Aspinwall *et al.*, 2019) and photosynthetic heat tolerance (T_{crit}) both in the field and under glasshouse conditions (Ghouil *et al.*, 2003; Zhu *et al.*, 2018). Thus, the general pattern appears to be that high T tolerance of both chloroplasts and mitochondria are strongly influenced by thermal history. If more widespread, this general acclimation pattern may help simplify the prediction of heat tolerance of leaf carbon metabolism to future climate warming scenarios

While thermal history is clearly a major factor driving variations in T_{max}, other factors such as air VPD and solar irradiance also appear to contribute. For example, at the FNQ_CT site (where summer is only marginally warmer than winter but is considerably wetter; Table 1), T_{max} was actually higher in the dry season (Fig. 3D). Dry (low humidity), bright conditions can result in reduced transpirational cooling which in turn leads to warming of leaves (Vogel, 2009). This may explain why in the stepwise regression analyses of data across all field sites and seasons, variations of T_{max} could be explained by variations in

growth T, F_n and VPD (Table 4). Past studies have reported that drought increases heat tolerance of R (e.g. increasing T_{max} by 6 °C in an evergreen tree species (Gauthier *et al.*, 2014)), with drought likely to have resulted in elevated canopy T (Blum *et al.*, 1989). Thus, high temperature tolerance of leaf R, while clearly influenced by growth T *per se*, is also influenced by other factors that co-occur with changes in leaf T. Future work needs to elucidate what factors are responsible for these changes in T_{max}, such as adjustments in membrane physical properties, and the abundance of key respiratory related protein complexes such as cytochrome *c* oxidase (Dahlhoff *et al.*, 1991; Dahlhoff & Somero, 1993; Sanmiya *et al.*, 2004), heat shock proteins and organic solutes (Vierling, 1991; Sung *et al.*, 2003). It also remains unknown why T_{max}, usually in the 50~60 °C range (O'Sullivan *et al.*, 2017; Zhu *et al.*, 2018), should consistently acclimate to sustained changes in (artificial) growth T often far beyond leaf T experienced in nature.

In conclusion, our study provides insights into the impact of contrasting environments on different elements derived from high-resolution *R*-*T* curves. We presented findings from 860 short-term *R*-*T* (10 – 70 °C range) curves measured on 62 species over two seasons in the field, with a third of those species then being grown under three common T regimes in controlled environments. Irrespective of whether plants were field or glasshouse grown, the *R*-*T* curves generally shifted in response to changes in growth T in a manner consistent with the thermal acclimation hypothesis outlined in Figure 1. This finding supports the incorporation of thermal acclimation of R_{25} into ecosystem models for a wide range of biomes. However, special attention may be needed for cool rainforest sites with extremely low light and low T. The ability of T_{max} to adjust to hot conditions – ensuring that mitochondria remain capable of producing the energy needed for cellular maintenance and biosynthesis - is likely to be of relevance to biome resilience in a future warmer and hotter world.

Acknowledgements

This work was funded by grants from the Australian Research Council Grants (DP0986823, DP130101252, CE140100008) to O. K. A. We also acknowledge the support of the Australian Government's Terrestrial Ecosystem Research Network (www.tern.org.au). We thank the support of staff at each site, including Matthias Boer, Matt Bradford, Peter Cale, James Cleverly, Craig Macfarlane, Wayne Meyer, Suzanne Prober, and Tim Wardlaw. We thank Dr. Terry Neeman (ANU Statistical Consulting Unit) for statistical advice. We also

thank the staff in ANU RSB Plant Services for professional plant care. The authors declare no conflict of interest.

Author contributions

OKA, KJB, KLG, VH, ML, PM, MHT and MGT planned and designed the field research. OKA and LZ planned and designed the glasshouse experiment. LZ, KJB, JJGE, LH, LKW and DC conducted fieldwork; LZ conducted glasshouse experiment. LZ, KJB, SA and OKA analysed data. LZ led the writing with substantial contributions from all authors.

Data availability statement

Data is available in TRY database (https://www.try-db.org/TryWeb/Home.php).

Supporting information

Figure S1 Example of two temperature response curves of leaf dark respiration (*R*-*T* curves).

Figure S2 Bar chart showing partitioning of variation in leaf mass per unit area (LMA), mass-based nitrogen concentration (N_m), area, mass and nitrogen-based leaf dark respiration measured at 25°C (R_{25a}, R_{25m} and R_{25n}), rate-temperature coefficients parameters (*b* and *c*) and temperature where leaf dark respiration reached the maximum (T_{max}).

Figure S3 Relationships between R_{25} or T_{max} and annual precipitation and annual mean temperature of species origins in a glasshouse study.

Table S1 List of the field sites surveyed in this study, including location, biome, vegetation types and climate data.

Table S2 Climatic description of each species provenances studied in glasshouse experiment.

Table S3 *R*-*T* parameters of species from four contrasting origins grown in a common environment as part of the glasshouse study Stage 1 experiment and results of one-way ANOVA.

Table S4 Linear regression analysis for *R*-*T* data relationships with environmental factors in the field.

Table S5 Linear regression analysis for *R*-*T* data relationships with environmental factors in the glasshouses.

References

Araki MG, Gyokusen K, Kajimoto T. 2017. Vertical and seasonal variations in temperature responses of leaf respiration in a *Chamaecyparis obtusa* canopy. *Tree Physiology* **37**: 1269-1284.

Arora V, Boer G, Friedlingstein P, Eby M, Jones C, Christian JR, Bonan GB, Bopp L, Brovkin V, Cadule P. 2013. Carbon-concentration and carbon-climate feedbacks in CMIP5 Earth system models. *Journal of Climate* **26**: 5289-5314.

Asao S, Hayes L, Aspinwall MJ, Rymer PD, Blackman C, Bryant CJ, Cullerne D, Egerton JJ, Fan Y, Innes P, et al. 2020. Leaf trait variation is similar among genotypes of *Eucalyptus camaldulensis* from differing climates and arises as plastic responses to the seasons rather than water availability. *New Phytologist* **227**: 780–793.

Aspinwall MJ, Drake JE, Campany C, Vårhammar A, Ghannoum O, Tissue DT, Reich PB, Tjoelker MG. 2016. Convergent acclimation of leaf photosynthesis and respiration to prevailing ambient temperatures under current and warmer climates in Eucalyptus tereticornis. *New Phytologist* **212**: 354-367.

Aspinwall MJ, Pfautsch S, Tjoelker MG, Vårhammar A, Possell M, Drake JE, Reich PB, Tissue DT, Atkin OK, Rymer PD. 2019. Range size and growth temperature influence *Eucalyptus* species responses to an experimental heatwave. *Global Change Biology* **25**: 1665-1684.

Atkin OK, Bloomfield KJ, Reich PB, Tjoelker MG, Asner GP, Bonal D, Bönisch G, Bradford MG, Cernusak LA, Cosio EG, et al. 2015. Global variability in leaf respiration in relation to climate, plant functional types and leaf traits. *New Phytologist* **206**: 614-636.

Atkin OK, Evans JR, Ball MC, Lambers H, Pons TL. 2000. Leaf respiration of snow gum in the light and dark. interactions between temperature and irradiance. *Plant Physiology* **122**: 915-923.

Atkin OK, Evans JR, Siebke K. 1998. Relationship between the inhibition of leaf respiration by light and enhancement of leaf dark respiration following light treatment. *Functional Plant Biology* **25**: 437-443.

Atkin OK, Tjoelker MG. 2003. Thermal acclimation and the dynamic response of plant respiration to temperature. *Trends in Plant Science* **8**: 343-351.

Bates D, Mächler M, Bolker B, Walker S. 2014. Fitting linear mixed-effects models using lme4. *arXiv preprint arXiv:1406.5823*.

Benomar L, Lamhamedi MS, Pepin S, Rainville A, Lambert M-C, Margolis HA, Bousquet J, Beaulieu J. 2017. Thermal acclimation of photosynthesis and respiration of southern and northern white spruce seed sources tested along a regional climatic gradient indicates limited potential to cope with temperature warming. *Annals of Botany* **121**: 443-457.

Beringer J, Hutley LB, McHugh I, Arndt SK, Campbell D, Cleugh HA, Cleverly J, Resco de Dios V, Eamus D, Evans B, et al. 2016. An introduction to the Australian and New Zealand flux tower network – OzFlux. *Biogeosciences* **13**: 5895-5916.

Bloomfield KJ, Prentice IC, Cernusak LA, Eamus D, Medlyn BE, Rumman R, Wright IJ, Boer MM, Cale P, Cleverly J. 2018. The validity of optimal leaf traits modelled on environmental conditions. *New Phytologist* **221**: 1409-1423.

Blum A, Shpiler L, Golan G, Mayer J. 1989. Yield stability and canopy temperature of wheat genotypes under drought-stress. *Field Crops Research* **22**: 289-296.

Bruhn D, Egerton JJG, Loveys BR, Ball MC. 2007. Evergreen leaf respiration acclimates to long-term nocturnal warming under field conditions. *Global Change Biology* **13**: 1216-1223.

Cunningham S, Read J. 2003. Comparison of temperate and tropical rainforest tree species: growth responses to temperature. *Journal of Biogeography* **30**: 143-153.

Dahlhoff E, O'Brien J, Somero GN, Vetter RD. 1991. Temperature effects on mitochondria from hydrothermal vent invertebrates: evidence for adaptation to elevated and variable habitat temperatures. *Physiological zoology* **64**: 1490-1508.

Dahlhoff E, Somero GN. 1993. Effects of temperature on mitochondria from abalone (*genus Haliotis*): adaptive plasticity and its limits. *Journal of Experimental Biology* **185**: 151-168.

Dillaway DN, Kruger EL. 2011. Leaf respiratory acclimation to climate: comparisons among boreal and temperate tree species along a latitudinal transect. *Tree Physiology* **31**: 1114-1127.

Drake JE, Furze ME, Tjoelker MG, Carrillo Y, Pendall E. 2019. Climate warming and tree carbon use efficiency in a whole‐tree $^{13}CO_2$ tracer study. *New Phytologist* **222**: 1313-1324.

Drake JE, Tjoelker MG, Aspinwall MJ, Reich PB, Barton CV, Medlyn BE, Duursma RA. 2016. Does physiological acclimation to climate warming stabilize the ratio of canopy respiration to photosynthesis? *New Phytologist* **211**: 850-863.

Dufresne J-L, Foujols M-A, Denvil S, Caubel A, Marti O, Aumont O, Balkanski Y, Bekki S, Bellenger H, Benshila R. 2013. Climate change projections using the IPSL-CM5 Earth System Model: from CMIP3 to CMIP5. *Climate Dynamics* **40**: 2123-2165.

Gauthier PPG, Crous KY, Ayub G, Duan H, Weerasinghe LK, Ellsworth DS, Tjoelker MG, Evans JR, Tissue DT, Atkin OK. 2014. Drought increases heat tolerance of leaf respiration in *Eucalyptus globulus* saplings grown under both ambient and elevated atmospheric CO_2 and temperature. *Journal of Experimental Botany* **65**: 6471-6485.

Ghouil H, Montpied P, Epron D, Ksontini M, Hanchi B, Dreyer E. 2003. Thermal optima of photosynthetic functions and thermostability of photochemistry in cork oak seedlings. *Tree Physiology* **23**: 1031-1039.

Heskel MA, O'Sullivan OS, Reich PB, Tjoelker MG, Weerasinghe LK, Penillard A, Egerton JJG, Creek D, Bloomfield KJ, Xiang J, et al. 2016. Convergence in the temperature response of leaf respiration across biomes and plant functional types. *Proceedings of the National Academy of Sciences* **113**: 3832-3837.

Huntingford C, Atkin OK, Martinez-de la Torre A, Mercado LM, Heskel MA, Harper AB, Bloomfield KJ, O'Sullivan OS, Reich PB, Wythers KR. 2017. Implications of improved representations of plant respiration in a changing climate. *Nature communications* **8**: 1602.

Hutchinson MF, McKenney DW, Lawrence K, Pedlar JH, Hopkinson RF, Milewska E, Papadopol P. 2009. Development and testing of Canada-wide interpolated spatial models of daily minimum–maximum temperature and precipitation for 1961–2003. *Journal of Applied Meteorology and Climatology* **48**: 725-741.

Hüve K, Bichele I, Ivanova H, Keerberg O, Parnik T, Rasulov B, Tobias M, Niinemets Ü. 2012. Temperature responses of dark respiration in relation to leaf sugar concentration. *Physiologia Plantarum* **144**: 320-334.

Karan M, Liddell M, Prober SM, Arndt S, Beringer J, Boer M, Cleverly J, Eamus D, Grace P, Van Gorsel E. 2016. The Australian SuperSite Network: A continental, long-term terrestrial ecosystem observatory. *Science of The Total Environment* **568**: 1263-1274.

Kruse J, Rennenberg H, Adams MA. 2011. Steps towards a mechanistic understanding of respiratory temperature responses. *New Phytologist* **189**: 659-677.

Li X, Xu C, Li Z, Feng J, Tissue DT, Griffin KL. 2019. Late growing season carbon subsidy in native gymnosperms in a northern temperate forest. *Tree Physiology* **39**: 1-12.

Liang LL, Arcus VL, Heskel MA, O'Sullivan OS, Weerasinghe LK, Creek D, Egerton JJG, Tjoelker MG, Atkin OK, Schipper LA. 2018. Macromolecular rate theory (MMRT) provides a thermodynamics rationale to underpin the convergent temperature response in plant leaf respiration. *Global Change Biology* **24**: 1538-1547.

Novozamsky I, Eck Rv, Van Schouwenburg JC, Walinga I. 1974. Total nitrogen determination in plant material by means of the indophenol-blue method. *Netherlands Journal of Agricultural Science* **22**: 3-5.

O'Sullivan OS, Heskel MA, Reich PB, Tjoelker MG, Weerasinghe LK, Penillard A, Zhu L, Egerton JJG, Bloomfield KJ, Creek D, et al. 2017. Thermal limits of leaf metabolism across biomes. *Global Change Biology* **23**: 209-223.

O'Sullivan OS, Weerasinghe KWLK, Evans JR, Egerton JJG, Tjoelker MG, Atkin OK. 2013. High-resolution temperature responses of leaf respiration in snow gum (*Eucalyptus pauciflora*) reveal high-temperature limits to respiratory function. *Plant Cell and Environment* **36**: 1268-1284.

Ow LF, Whitehead D, Walcroft AS, Turnbull MH. 2010. Seasonal variation in foliar carbon exchange in *Pinus radiata* and *Populus deltoides*: respiration acclimates fully to changes in temperature but photosynthesis does not. *Global Change Biology* **16**: 288-302.

Padfield D, Yvon‐Durocher G, Buckling A, Jennings S, Yvon‐Durocher G. 2016. Rapid evolution of metabolic traits explains thermal adaptation in phytoplankton. *Ecology Letters* **19**: 133-142.

Quan X, Wang C. 2018. Acclimation and adaptation of leaf photosynthesis, respiration and phenology to climate change: A 30-year *Larix gmelinii* common-garden experiment. *Forest Ecology and Management* **411**: 166-175.

R Development Core Team R. 2020. R: A language and environment for statistical computing. R Foundation for Statistical Computing, Vienna, Austria. *Online: http://www. R-project. org*.

Reich PB, Sendall KM, Stefanski A, Wei X, Rich RL, Montgomery RA. 2016. Boreal and temperate trees show strong acclimation of respiration to warming. *Nature* **531**: 633-636.

Sanmiya K, Suzuki K, Egawa Y, Shono M. 2004. Mitochondrial small heat-shock protein enhances thermotolerance in tobacco plants. *Febs Letters* **557**: 265-268.

Searle SY, Thomas S, Griffin KL, Horton T, Kornfeld A, Yakir D, Hurry V, Turnbull MH. 2011. Leaf respiration and alternative oxidase in field‐grown alpine grasses respond to natural changes in temperature and light. *New Phytologist* **189**: 1027-1039.

Searle SY, Turnbull MH. 2011. Seasonal variation of leaf respiration and the alternative pathway in field‐grown *Populus*× *canadensis*. *Physiologia Plantarum* **141**: 332-342.

Slot M, Kitajima K. 2015. General patterns of acclimation of leaf respiration to elevated temperatures across biomes and plant types. *Oecologia* **177**: 885-900.

Smith NG, Dukes JS. 2013. Plant respiration and photosynthesis in global-scale models: incorporating acclimation to temperature and CO_2. *Global Change Biology* **19**: 45-63.

Smith NG, Malyshev SL, Shevliakova E, Kattge J, Dukes JS. 2015. Foliar temperature acclimation reduces simulated carbon sensitivity to climate. *Nature Climate Change* **6**: 407.

Strain B. 1969. Seasonal adaptations in photosynthesis and respiration in four desert shrubs growing in situ. *Ecology* **50**: 511-513.

Sung DY, Kaplan F, Lee KJ, Guy CL. 2003. Acquired tolerance to temperature extremes. *Trends in Plant Science* **8**: 179-187.

Tjoelker MG, Oleksyn J, Lorenc‐Plucinska G, Reich P. 2009. Acclimation of respiratory temperature responses in northern and southern populations of *Pinus banksiana*. *New Phytologist* **181**: 218-229.

Turnbull MH, Ogaya R, Barbeta A, Peñuelas J, Zaragoza-Castells J, Atkin OK, Valladares F, Gimeno TE, Pías B, Griffin KL. 2017. Light inhibition of foliar respiration in response to soil water availability and seasonal changes in temperature in Mediterranean holm oak (*Quercus ilex*) forest. *Functional Plant Biology* **44**: 1178-1193.

Vanderwel MC, Slot M, Lichstein JW, Reich PB, Kattge J, Atkin OK, Bloomfield KJ, Tjoelker MG, Kitajima K. 2015. Global convergence in leaf respiration from estimates of thermal acclimation across time and space. *New Phytologist* **207**: 1026-1037.

Vierling E. 1991. The roles of heat-shock proteins in plants. *Annual Review of Plant Physiology and Plant Molecular Biology* **42**: 579-620.

Vogel S. 2009. Leaves in the lowest and highest winds: temperature, force and shape. *New Phytologist* **183**: 13-26.

Way DA, Holly C, Bruhn D, Ball MC, Atkin OK. 2015. Diurnal and seasonal variation in light and dark respiration in field-grown *Eucalyptus pauciflora*. *Tree Physiology* **35**: 840-849.

Wright IJ, Reich PB, Atkin OK, Lusk CH, Tjoelker MG, Westoby M. 2006. Irradiance, temperature and rainfall influence leaf dark respiration in woody plants: evidence from comparisons across 20 sites. *New Phytologist* **169**: 309-319.

Wright IJ, Reich PB, Westoby M, Ackerly DD, Baruch Z, Bongers F, Cavender-Bares J, Chapin T, Cornelissen JHC, Diemer M, et al. 2004. The worldwide leaf economics spectrum. *Nature* **428**: 821-827.

Xu T, Hutchinson M. 2011. ANUCLIM version 6.1 user guide. *The Australian National University, Fenner School of Environment and Society, Canberra*.

Zaragoza-Castells J, Sanchez-Gomez D, Valladares F, Hurry V, Atkin OK. 2007. Does growth irradiance affect temperature dependence and thermal acclimation of leaf respiration? Insights from a Mediterranean tree with long-lived leaves. *Plant Cell and Environment* **30**: 820-833.

Zhu L, Bloomfield KJ, Hocart CH, Egerton JJG, O'Sullivan OS, Penillard A, Weerasinghe LK, Atkin OK. 2018. Plasticity of photosynthetic heat tolerance in plants adapted to thermally contrasting biomes. *Plant Cell & Environment* **41**: 1251-1262.

Table 1. Seasonal climatic description for each field campaign.

Site	Season	Month/Year	Mean temperature °C	Mean max temperature °C	Max temperature recorded °C	Precipitation mm	F_n W m^{-2}	VPD kPa	Sws fraction
Cape Tribulation, Far North Queensland (FNQ_CT)	Dry	Sep 2010	24.4	27.5	29.7	209.6	85.5	0.62	-
	Wet	Mar 2014	25.0	27.2	31.1	1,287.2	90.9	0.63	0.385
Robson Creek, Far North Queensland (FNQ_RC)	Dry	Aug 2012	17.2	21.6	26.1	46.0	64.0	0.34	-
	Wet	Apr 2014	21.8	26.2	28.0	238.3	129.5	0.38	0.325
Alice Mulga, Northern Territory (NT_AM)	Summer	Feb 2013	30.2	37.2	42.2	10.2	166.9	3.47	0.034
	Winter	Aug 2014	15.5	22.0	25.9	0.0	92.9	1.29	0.059
Great Western Woodland, Western Australia (WA_GWW)	Summer	Apr 2013	23.5	30.0	37.2	26.4	116.2	1.89	0.209
	Winter	Aug 2013	14.7	20.1	29.0	27.2	83.1	0.83	0.117
Cumberland Plain, New South Wales (NSW_CP)	Summer	Jan 2014	23.8	30.7	39.5	13.2	180.4	1.15	0.054
	Winter	Jul 2014	12.3	18.5	21.5	7.0	52.6	0.62	0.052
Warra, Tasmania (TAS_WAR)	Summer	Mar 2012	15.9	21.6	36.5	72.9	106.2	0.52	-
	Winter	Jun 2013	6.6	9.8	14.5	57.6	6.4	0.21	0.178

All climatic variables were calculated using mean data from the 30 days prior to the date of measurement. In most cases the climate data have been obtained from flux towers located at each site (TERN Ozflux, www.ozflux.org.au). In two cases (FNQ_RC dry season and TAS_WAR summer season) interpolated data were used obtained from

ANUCLIM (TERN eMAST, https://www.tern.org.au/) and radiation data were obtained from the nearest weather station operated by the Australian Bureau of Meteorology (www.bom.gov.au). Abbreviations: F_n: Net radiation; VPD: vapor pressure deficit; Sws: soil water fraction of top layer.

Table 2. Linear mixed model and analysis of variance results of *R*-*T* parameters and leaf traits of six sites where measurements were made in both seasons in the field.

	Site		Season		Site × Season	
	F	*P*	*F*	*P*	*F*	*P*
LMA	7.22	< 0.001	1.63	0.203	10.34	< 0.001
N_m	3.68	0.004	1.83	0.178	4.17	0.003
R_{25a}	12.35	< 0.001	15.81	< 0.001	18.03	< 0.001
R_{25m}	3.59	0.005	6.08	0.014	10	< 0.001
R_{25n}	3.59	0.005	6.69	0.001	12.51	< 0.001
b	0.87	0.503	1.91	0.168	7.89	< 0.001
c	0.81	0.549	1.21	0.271	3.76	0.003
T_{max}	6.51	< 0.001	65.5	< 0.001	6.91	< 0.001

LMA: leaf mass per unit leaf dry area, g m^{-2}; N_m: leaf nitrogen per unit mass, mg g^{-1}; R_{25a}: Respiration rate at 25 °C on leaf area bases, μmol CO_2 m^{-2} s^{-1}; R_{25m}: Respiration rate at 25 °C on leaf mass bases, nmol CO_2 g^{-1} s^{-1}; R_{25n}: Respiration rate at 25 °C on nitrogen bases, nmol CO_2 gN^{-1} s^{-1}; *b* and *c*: rate-temperature coefficients; T_{max}: leaf temperature where respiration reaches its maximum, °C.

Table 3. Impact of growth temperature treatment (20/15 °C, day/night temperatures; 30/25 °C) on *R-T* parameters and leaf traits (LMA, N_m) of plants sourced from four Australian biomes.

	Origin		Treatment		Origin × Treatment	
	F	*P*	*F*	*P*	*F*	*P*
LMA	22.21	< 0.001	22.27	< 0.001	0.10	0.959
N_m	13.04	< 0.001	0.71	0.401	0.05	0.987
R_{25a}	36.49	< 0.001	48.47	< 0.001	1.04	0.376
R_{25m}	10.50	< 0.001	8.00	0.029	0.60	0.618
R_{25n}	7.78	< 0.001	29.83	0.002	1.44	0.236
b	2.92	0.037	1.08	0.301	0.79	0.500
c	3.89	0.011	1.72	0.191	1.03	0.382
T_{max}	0.89	0.447	28.18	< 0.001	0.68	0.565

LMA: leaf mass per unit leaf dry area, g m^{-2}; N_m: leaf nitrogen per unit mass, mg g^{-1}; R_{25a}: Respiration rate at 25 °C on leaf area bases, μmol CO_2 m^{-2} s^{-1}; R_{25m}: Respiration rate at 25 °C on leaf mass bases, nmol CO_2 g^{-1} s^{-1}; R_{25n}: Respiration rate at 25 °C on nitrogen bases, nmol CO_2 gN^{-1} s^{-1}; *b* and *c*: rate-temperature coefficients; T_{max}: leaf temperature where respiration reaches its maximum, °C. Shown are two-way analysis of variance results of the glasshouse Stage 2 experiment. See Table S3 for Stage 1 results.

Table 4. Stepwise multiple regression analysis of relationships between R_{25a} or T_{max} and climate factors in the field.

Final model	r^2	P	Intercept *t*-value (*P* value)	mean*T* *t*-value (*P* value)	F_n *t*-value (*P* value)	VPD *t*-value (*P* value)
Initial model: log(R_{25a}) or T_{max} = β0 + β1*log(mean*T*) + β2 * log(F_n) + β3 * log(VPD) + β4 * log(PPT)						
log(R_{25a}) All sites - seasons log(R_{25a}) = 0.56 - 0.58*log(mean*T*) + 0.58 * log(F_n) + 0.32 * log(VPD)	0.3054	< 0.001	3.019 (0.003)	-5.556 (< 0.001)	4.425 (< 0.001)	3.339 (0.001)
TAS_WAR summer and winter excluded log(R_{25a}) = 1.38 - 0.46*log(mean*T*) + 0.41 * log(VPD)	0.2976	< 0.001	5.754 (< 0.001)	-5.938 (< 0.001)		4.661 (< 0.001)
TAS_WAR winter excluded log(R25a) = 1.36 - 0.46*log(meanT) + 0.41 * log(VPD)	0.2884	< 0.001	5.867 (< 0.001)	-6.048 (< 0.001)		4.789 (< 0.001)
T_{max} All sites - seasons T_{max} = 47.96 + 6.26*log(mean*T*) - 4.37 * log(F_n) +2.26 * log(VPD)	0.2976	< 0.001	22.364 (< 0.001)	5.545 (< 0.001)	-2.846 (0.005)	2.64 (0.027)

Mean T, F_n, VPD and PPT are mean temperature, mean net radiation, mean vapor pressure deficit and total precipitation of 30 days prior to the date of measurements. The t-value and P-value for each coefficient indicates significance.

Figure legends

Figure 1. Schematic graph on acclimation of the short-term temperature response curve of leaf dark respiration (*R*-*T* curve) to sustained differences in growth temperature (cold grown vs. warm grown). Parameters used to describe the shift of *R*-*T* curve: (1) shift of the elevation – *R* at a set *T*, e.g. R_{25} (*R* at temperature 25°C represents *R* under biologically-relevant temperatures); (2) shift of the temperature where respiration reaches the maximum value (T_{max}, represents thermal threshold of *R*); (3) changes of the rate-temperature coefficients, e.g., *b* and *c* from the Global Polynomial Model (GPM) for respiration (Heskel *et al.*, 2016), or the overall activation energy of respiratory processes based on Arrhenius equation (E_a), or the rate of change of respiration rate through increasing the temperature by 10°C (Q_{10}) (Kruse *et al.*, 2011). Here in our study, GPM was applied and the rate-temperature coefficients were derived using *R*-*T* curve where *T* was below 45°C. Based on previous studies (Atkin & Tjoelker 2003, Slot & Kitajima 2015), *R*-*T* curves from plants growing in cold and warm temperatures will show thermal acclimation. Under warming scenarios, R_{25} would be down-regulated toward homeostasis and T_{max} would increase, indicating the increase of respiratory heat tolerance. The temperature coefficients would stay the same, reflecting no changes in temperature sensitivity. In this study, R_{25} values are presented on area, mass and nitrogen bases.

Figure 2. Variations of leaf mass per unit area (LMA, a) and mass-based nitrogen concentration (N_m, b) in two seasons (cool and warm seasons) across six field sites, and in plants sourced from four climatic origins close to field sites to two growth temperature treatments in Stage 2 glasshouse study (c, d). For field sites: FNQ_CT, Cape Tribulation in tropical wet forest Far North Queensland; FNQ_RC, Robson Creek in tropical wet forest Far North Queensland; NT_AM, Alice Mulga in the woodland of Northern Territory; WA_GWW, Greater Western Woodland in semi-arid woodland, Western Australia; NSW_CP, Cumberland Plain in temperate woodland of New South Wales; TAS_WAR, Warra in a cool-temperate wet forest in Tasmania. Cool and warm seasons are dry and wet seasons in the two tropical rainforest sites (FNQ_CT and FNQ_RC) and winter and summer seasons for the other four sites. For glasshouse plant origins: FNQ represents tropical rainforest in Far North Queensland, WA for Mediterranean woodland in Western Australia, NSW for temperate forest in New South Wales and TAS for temperate rainforest in Tasmania. The vertical line indicates the 10th to the 90th percentile ranges and the horizontal line within box is the median value. '*' represents significant differences at $P < 0.05$.

Figure 3. Variations of area (R_{25a}, a), mass (R_{25m}, b) and nitrogen-based (R_{25n}, c) rates of leaf dark respiration measured at 25 °C, temperature where leaf *R* reached maximum rates (T_{max}, d), rate-temperature coefficients *b* (e) and *c* (f), and in two seasons (cool and warm seasons) across six field sites FNQ_CT, Cape Tribulation in tropical wet forest Far North Queensland; FNQ_RC, Robson Creek in tropical wet forest Far North Queensland; NT_AM, Alice Mulga in the woodland of Northern Territory; WA_GWW, Greater Western Woodland in semi-arid woodland, Western Australia; NSW_CP, Cumberland Plain in temperate woodland of New South Wales; TAS_WAR, Warra in a cool-temperate wet forest in Tasmania. Cool and warm seasons are designated, respectively, dry and wet seasons in the two tropical rainforest sites (FNQ_CT and FNQ_RC) and winter and summer seasons for the other four sites. The vertical line indicates the 10th to the 90th percentile ranges and the horizontal line within box is the median value. '*' represents significant differences at $P < 0.05$.

Figure 4. Relationships between R_{25a} (a, b, c and d) and T_{max} (e, f, g and h) and seasonal changes of mean temperature (mean T), net radiation (F_n), vapor pressure deficit (VPD) and precipitation (PPT) of the 30 day period prior to the date of measurements (PDM) in the field across two contrasting seasons of six thermally contrasting field sites. Where shown, lines represent significant linear regressions across two contrasting seasons. Dashed line represents cool season and solid line represents warm season. Linear regressions between R_{25a} and PPT, between T_{max} and mean T or F_n shared same intercepts and slopes between cool and warm seasons. Linear regressions between and R_{25a} and F_n or PPT, between T_{max} and VPD shared same slopes but different intercepts between the two seasons. Details of linear regressions can be found in Table S4. In addition, stepwise regressions were performed to look at relationships between R_{25a} or T_{max} and the four climate factors and results are shown in Table 4.

Figure 5. Variations of area (R_{25a}, a), mass (R_{25m}, b) and nitrogen-based (R_{25n}, c) leaf dark respiration measured at 25 °C, temperature where leaf R reached maximum rates (T_{max}, d), rate-temperature coefficients b (e) and c (f), and in Stage 2 of the glasshouse study. FNQ represents tropical rainforest in Far North Queensland, WA for Mediterranean woodland in Western Australia, NSW for temperate forest in New South Wales and TAS for temperate rainforest in Tasmania. The vertical line indicates the 10^{th} to the 90^{th} percentile ranges and the horizontal line within box is the median value. '*' represents significant differences at $P < 0.05$.

Figure 6. Predicted species response patterns from linear mixed-effects models of (a) R_{25a} and (b) T_{max} to growth temperature (T). Each point represents an individual plant; each line shows a regression between the y-axis parameter and growth T for each species, with regressions fitted using individual plant data of each species at low and high growth Ts. For field data, growth T represents seasonal changes of mean temperature (mean T) of 30 days prior to the date of measurements; for glasshouse data, growth T was calculated from the mean of each T treatment.

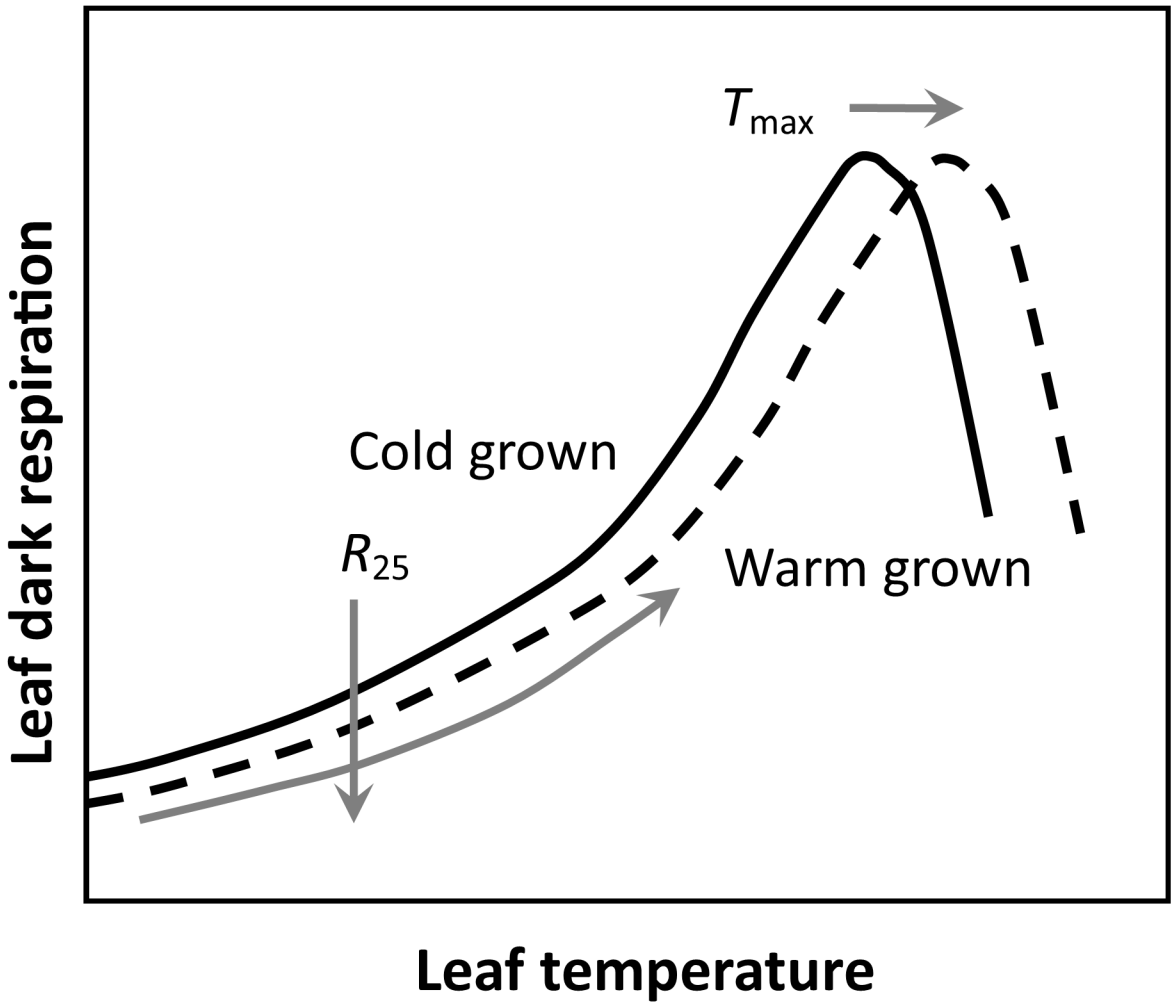

nph_16929_f1.tif

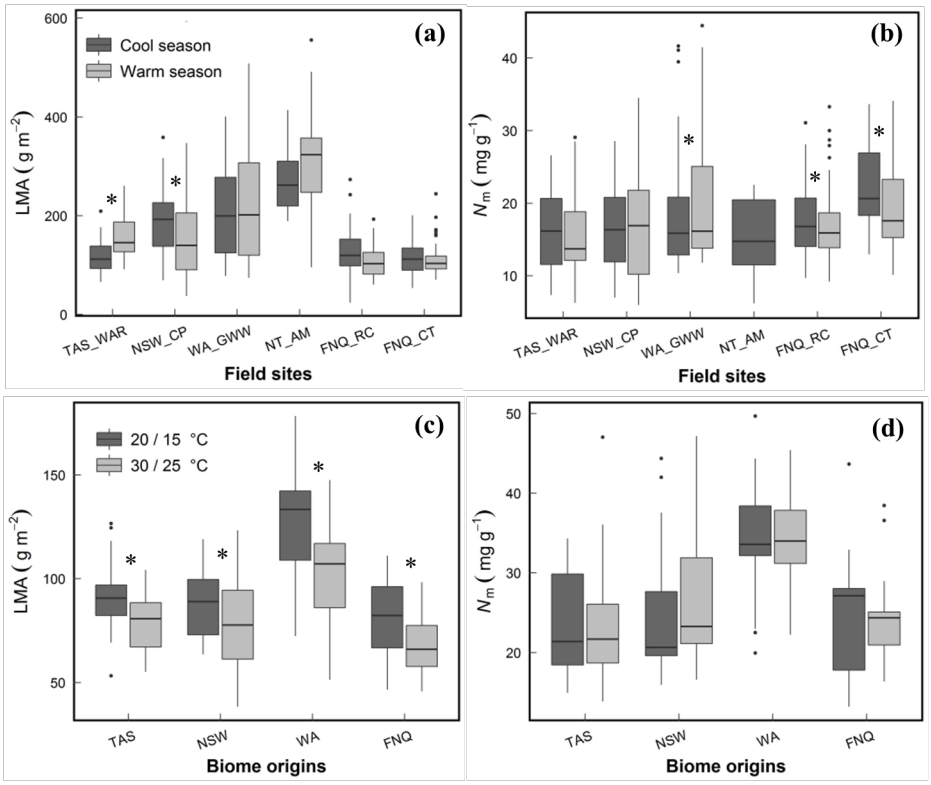

nph_16929_f2.tif

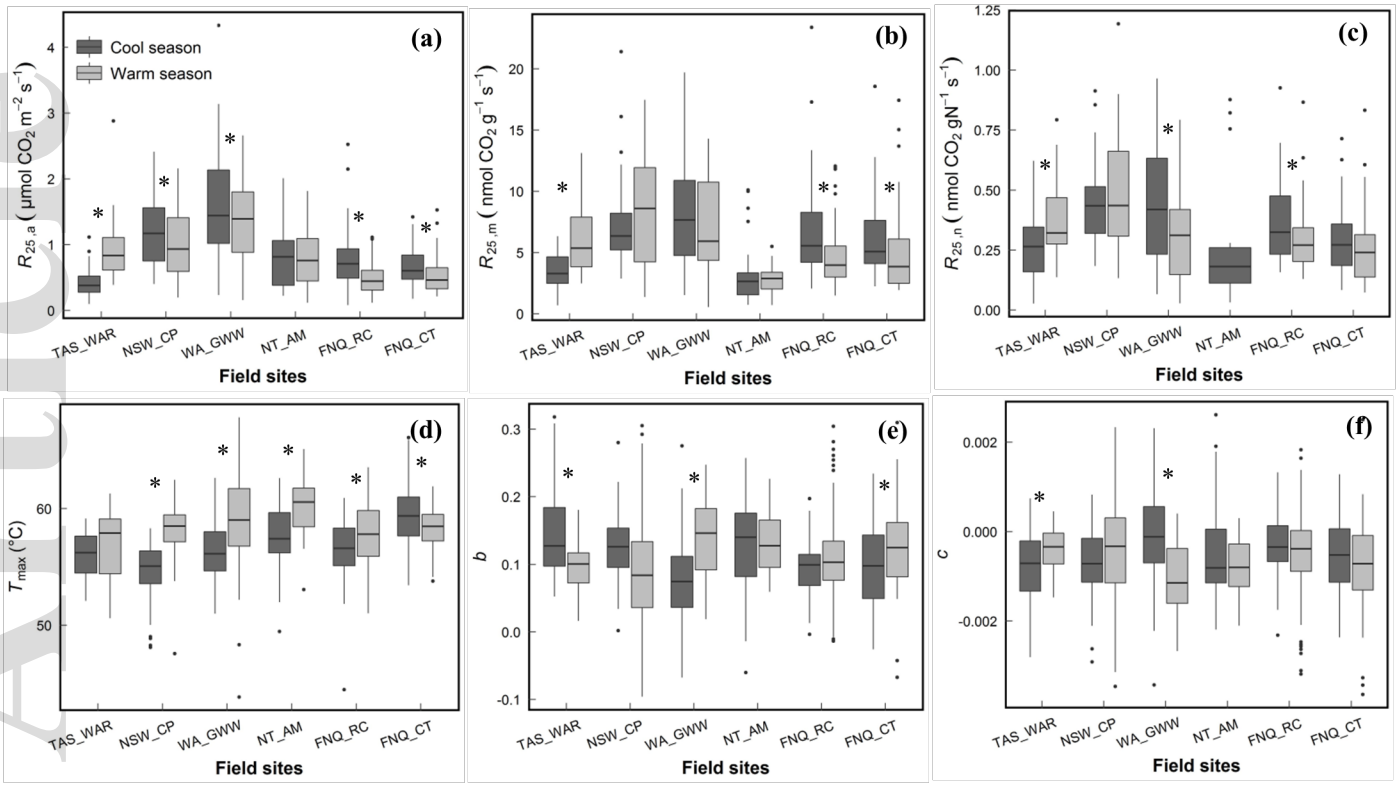

nph_16929_f3.tif

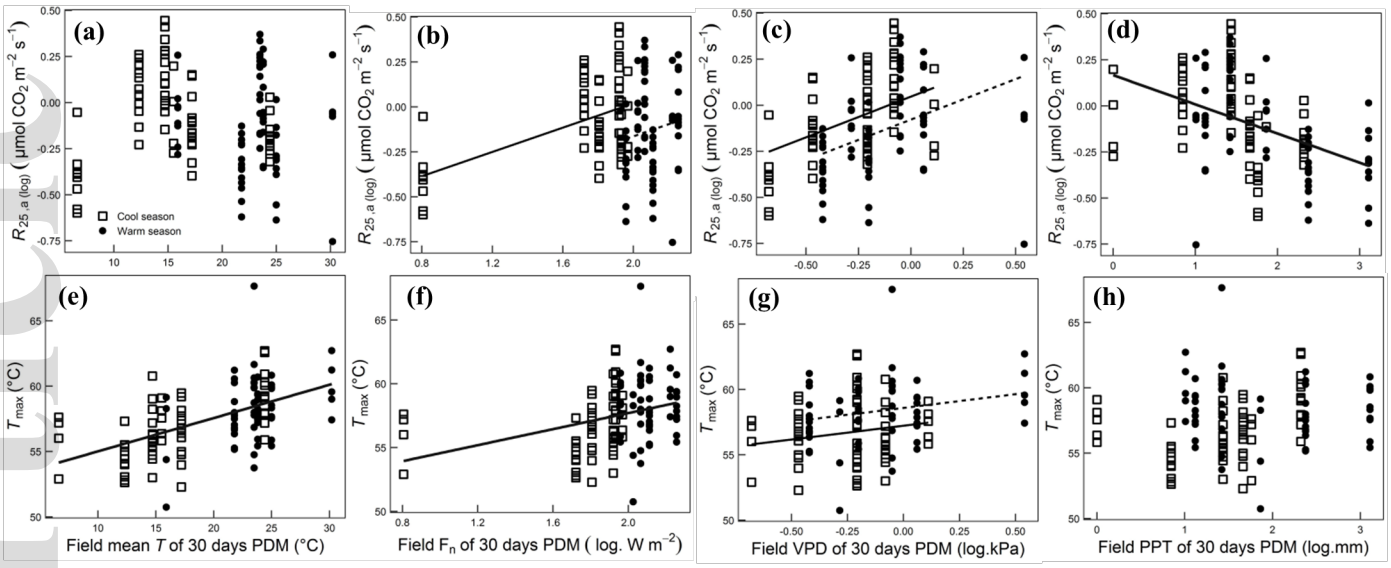

nph_16929_f4.tif

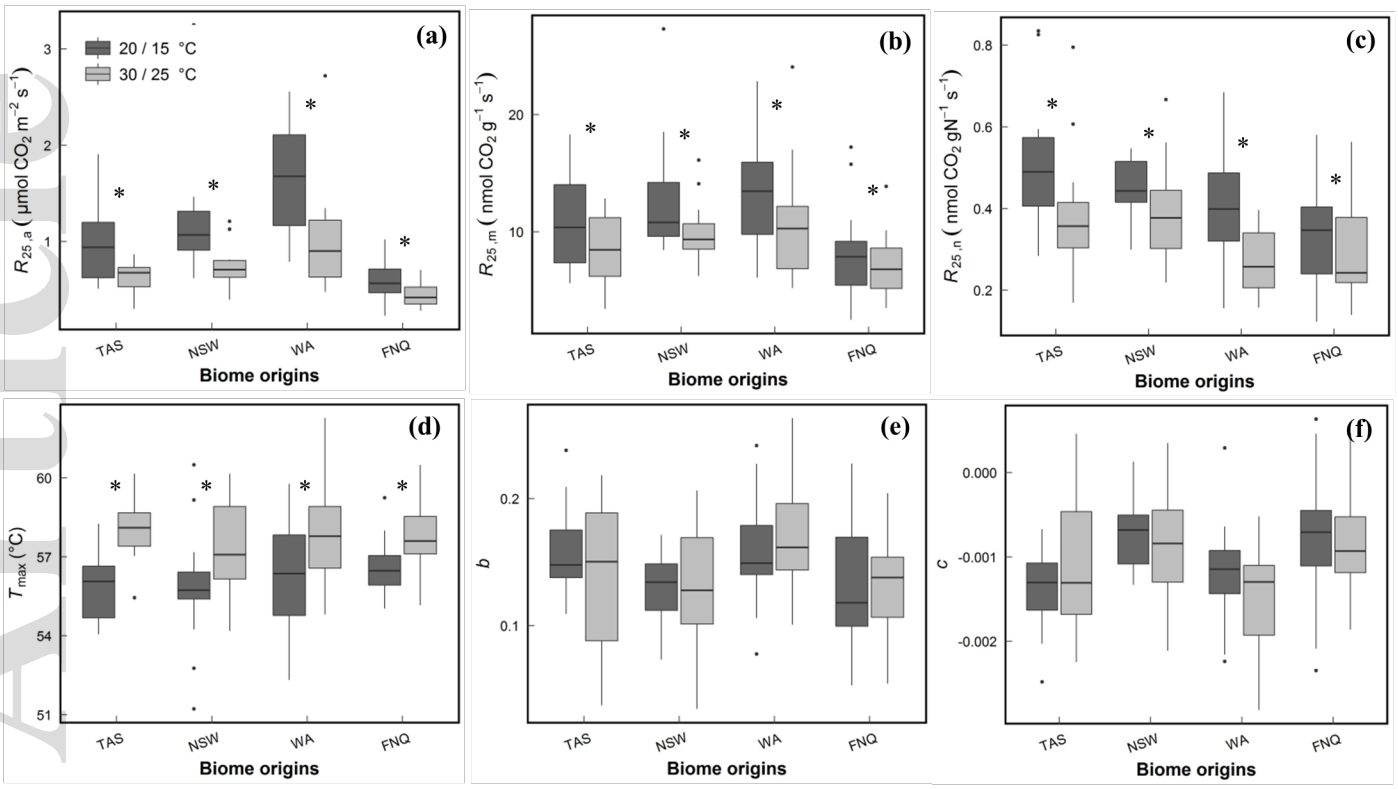

nph_16929_f5.tif

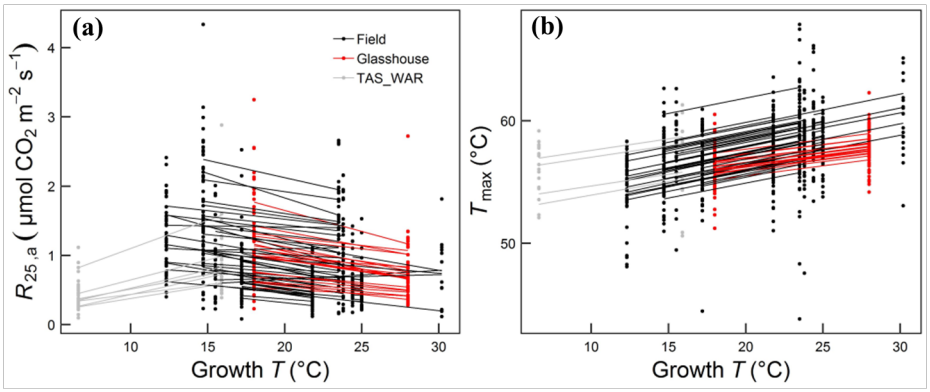

nph_16929_f6.tif